

## Amino substituted 4-pyridylbutadienes: Synthesis and fluorescence investigations

Harsha Agnihotri <sup>b</sup>, Paramasivam Mahalingavelar <sup>b</sup>, Hemant Mande <sup>a</sup>, Prasanna Ghalsasi <sup>a</sup>, Sriram Kanvah <sup>b,\*</sup>

<sup>a</sup> Department of Chemistry, MS University of Baroda, Pratapgunj, Vadodara, Gujarat 390002, India

<sup>b</sup> Department of Chemistry, Indian Institute of Technology Gandhinagar, Chandkheda, Ahmedabad 382 424, India

### ARTICLE INFO

#### Article history:

Received 4 May 2015

Received in revised form

27 July 2015

Accepted 17 August 2015

Available online 25 August 2015

#### Keywords:

Solvatochromism

Pyridyl dyes

Donor-acceptor systems

Julolidine

Intramolecular charge transfer

Diarylpolyenes

### ABSTRACT

Synthesis and spectroscopic investigations of a series of donor- $\pi$ -acceptor systems containing pyridine as the electron withdrawing group and an amino derivative (dimethylamino, diphenylamino, carbazole and julolidine) as electron donating group, separated by a  $\pi$ -spacer are described. The effect of varying donors on absorption and emission properties was studied in different solvents. All the molecules investigated exhibit pronounced positive polarity dependent solvatochromic shifts of up to ~141 nm. Strong fluorescence quantum yields are also observed for dienes containing carbazole and diphenylamine donors. This behavior suggests the presence of highly polar emitting states as a result of  $\pi$ - $\pi^*$  intramolecular charge-transfer (ICT). The observations were corroborated by a linear relation of the fluorescence maximum ( $\lambda_{max}$ ) versus the solvent polarity function ( $\Delta_f$ ) from the Lippert–Mataga correlation. The emission lifetime shows a decay profile consistent with the formation of one species (**1** and **3**) and two species (**2** and **4**) in the excited state.

© 2015 Elsevier Ltd. All rights reserved.

## 1. Introduction

$\pi$ -conjugated substrates bearing  $\pi$ -electron donor (D) and a  $\pi$ -electron acceptor substitutions exhibiting intramolecular charge transfer (ICT) have gained prominence for use as functional organic materials [1–6]. Among many known substrates, derivatives such as donor-acceptor substituted diphenylpolyenes have attracted attention as model compounds to understand the light induced conformational processes of biological substrates [7] and also as fluorescence probes [8]. Replacement of CH of the phenyl ring of diphenylpolyenes by nitrogen (N) leads to an isoelectronic species that is expected to have significant influence on the electronic properties due to the presence of (n,  $\pi^*$ ) states [9]. Consequently, neutral styryl and butadienyl pyridine analogs have been synthesized and were investigated for their solution and/or solid state photochemical [10–12] and photophysical properties [13–15]. Examples of photochemical investigations include regioselective photodimerization [16,17], formation of pre-organized molecular ladderane like structures through hydrogen bonding interactions [18] and photoisomerization studies [10,12,14]. Apart from its role

towards photochemical transformations, the lone pair of electrons on the nitrogen atom of the pyridine contributes to a coordinate covalent bonding with Lewis acid sites of TiO<sub>2</sub> surface lending its utility as anchoring group for dye-sensitized solar cells applications [19–21]. Because of the facile protonation of pyridine moiety and its role in deactivating effect of the (n,  $\pi^*$ ) state [22], these substrates have also been utilized as potential fluorescence probes for biological applications [23–28] and also for non-linear optical (NLO) applications [29,30]. In contrast to research investigations on unsubstituted pyridylbutadiene derivatives, the emission properties of the electron donor or acceptor substituted heterocyclic (pyridine) derivatives of butadienes are scarce. Here in, we report synthesis and solvatochromic properties of novel amino [dimethylamino, diphenylamino, carbazole and julolidine] substituted 4-pyridylbutadiene derivatives (Fig. 1). Through this study, we also intend to examine influence of extended  $\pi$ -conjugation on the steady state and time resolved emission properties of the substrates. The results suggest remarkable fluorescence properties characterized by intramolecular charge transfer (ICT).

## 2. Experimental

The reagents required for the synthesis of pyridyl substituted derivatives were obtained from Sigma–Aldrich, Alfa Aesar, Acros

\* Corresponding author.

E-mail addresses: [kanvah@gatech.edu](mailto:kanvah@gatech.edu), [sriram@iitgn.ac.in](mailto:sriram@iitgn.ac.in) (S. Kanvah).

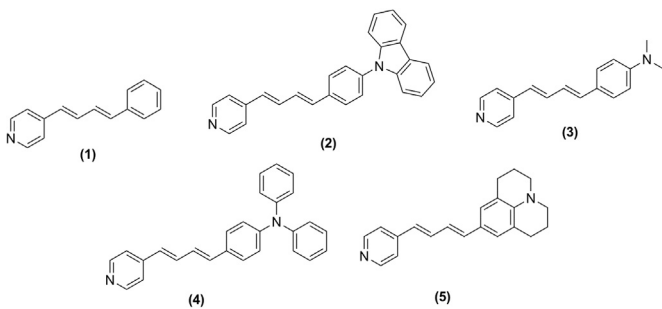


**Fig. 1.** Structures of synthesized 4-pyridyl-4-phenylbutadiene derivatives.

and S.D. Fine. The solvents utilized for the synthesis and spectral studies were dried using reported procedures.  $^1\text{H}$  and  $^{13}\text{C}$  NMR spectra were carried out using 500 MHz Bruker Avance spectrometer in  $\text{CDCl}_3$  with tetramethylsilane as an internal standard. Accurate mass analysis was performed using Waters-Synapt G2S (ESI-QToF) mass spectrometer. Absorption spectra were recorded on Analytik Jena, Specord 210 model UV-vis spectrophotometer. Steady state fluorescence studies were performed utilizing Horiba Jobin-Yvon fluorolog-3 spectrofluorimeter and relative fluorescence quantum yields were measured using quinine sulfate (0.545 in 0.5 N  $\text{H}_2\text{SO}_4$ ) as a standard [31]. The concentrations used for fluorescence experiments are typically in the order of  $10^{-5}$  M. The excitation wavelengths were set at the absorption maxima ( $\lambda_a$ ) of the compounds while recording their emission spectra. Fluorescence life-times were determined by Edinburgh Life Spec II instrument at excitation wavelengths of 360 nm for (2), 405 nm for (3–5). The percent error associated with the lifetime studies is 0.1–0.3%.

## 2.1. X-ray crystallographic details

Crystallographic data for the compound (4) was collected on Xcalibur, Gemini with EOS detector diffractometer. The reflection data was integrated and reduced using CrysAlisPro and Superflip [32] and the structure was refined using SHELLSX97 [33]. ORTEP diagrams of the compound generated using ORTEP-3. The single crystals of (4) were grown in acetone solvent system. The crystallographic data reveal that the compound (4) crystallized into a triclinic crystal system with space group P-1 with  $Z = 2$  and shows a *trans*-configuration. Crystallographic data and the ORTEP diagram are given in the supporting information [Tables C1–C3 and Fig. C1].

## 2.2. Synthesis of (1), (3), (4) and (5)

The synthetic scheme for the preparation of dienes (1), (3–5) is given in Scheme 1c. In a typical procedure [15], a mixture of diphenyl (4-picolylophosphane oxide [34] (1 equiv), NaH (2.5 equiv), 18-crown-6 (0.5 equiv) was stirred in 40 mL of dry THF at 0 °C. After 30 min of stirring, 4-substituted cinnamaldehyde (1 equiv) in dry THF was added drop wise and allowed to stir for 10 h at room temperature. The reaction mixture was then filtered over celite and the desired product was purified by column chromatography using neutral silica gel using 30% ethyl acetate/petroleum ether.

### 2.2.1. *N,N*-dimethyl-4-((1E,3E)-4-(pyridin-4-yl)buta-1,3-dienyl) aniline (3)

Brown solid,  $^1\text{H}$  NMR ( $\text{CDCl}_3$ , 500 MHz, ppm)  $\delta$  8.50 (d, 2H),  $\delta$  7.36–7.35 (d, 2H),  $\delta$  7.15–7.09 (dd, 1H,  $J = 15.5$  Hz),  $\delta$  6.80–6.68 (m, 4H),  $\delta$  6.47–6.44 (d, 1H,  $J = 15.5$  Hz),  $\delta$  2.99 (s, 6H);  $^{13}\text{C}$  NMR ( $\text{CDCl}_3$ ,

125 MHz, ppm)  $\delta$  150.56, 149.89, 136.54, 134.68, 128.03, 126.95, 123.93, 120.42, 112.29, 40.34. HRMS [M+1]<sup>+</sup> 251.1550.

### 2.2.2. *N,N*-diphenyl-4-((1E,3E)-4-(pyridin-4-yl)buta-1,3-dienyl) aniline (4)

Yellow solid,  $^1\text{H}$  NMR ( $\text{CDCl}_3$ , 500 MHz, ppm)  $\delta$  8.51–8.50 (d, 2H),  $\delta$  7.32–7.26 (m, 8H),  $\delta$  7.14–7.09 (m, 5H),  $\delta$  7.05–7.00 (m, 4H),  $\delta$  6.86–6.80 (m, 1H,  $J = 15.5$  Hz),  $\delta$  6.73–6.70 (d, 1H,  $J = 15.5$  Hz),  $\delta$  6.53–6.49 (d, 1H,  $J = 15.5$  Hz);  $^{13}\text{C}$  NMR ( $\text{CDCl}_3$ , 125 MHz, ppm)  $\delta$  149.96,  $\delta$  148.06,  $\delta$  147.36,  $\delta$  144.9,  $\delta$  135.56,  $\delta$  134.06,  $\delta$  130.58,  $\delta$  129.36,  $\delta$  128.58,  $\delta$  127.65,  $\delta$  126.39,  $\delta$  124.81,  $\delta$  123.39,  $\delta$  123.02, 120.54. HRMS [ESI] [M+1]<sup>+</sup> 375.1859.

### 2.2.3. 9-((1E,3E)-4-(pyridin-4-yl)buta-1,3-dienyl)-1,2,3,5,6,7-hexahydropyrido[3,2,1-ij]quinoline (5)

Brown solid;  $^1\text{H}$  NMR ( $\text{CDCl}_3$ , 500 MHz, ppm)  $\delta$  8.48–8.47 (d, 2H), 7.23–7.22 (2H, d), 7.12–7.07 (m, 1H,  $J = 15.5$  Hz), 6.91 (s, 2H), 6.73–6.68 (m, 1H,  $J = 15.5$  Hz), 6.62–6.59 (d, 1H,  $J = 15$  Hz), 6.42–6.39 (d, 1H,  $J = 15$  Hz), 3.19–3.17 (4H, t), 2.76–2.73 (4H, t), 1.97–1.95 (4H, t);  $^{13}\text{C}$  NMR ( $\text{CDCl}_3$ , 125 MHz, ppm)  $\delta$  151.7, 149.8, 145.4, 143.3, 136.9, 134.8, 126.2, 125.8, 124.0, 123.0, 121.2, 120.3, 49.9, 27.7, 21.8 HRMS [M+1]<sup>+</sup> 303.1868.

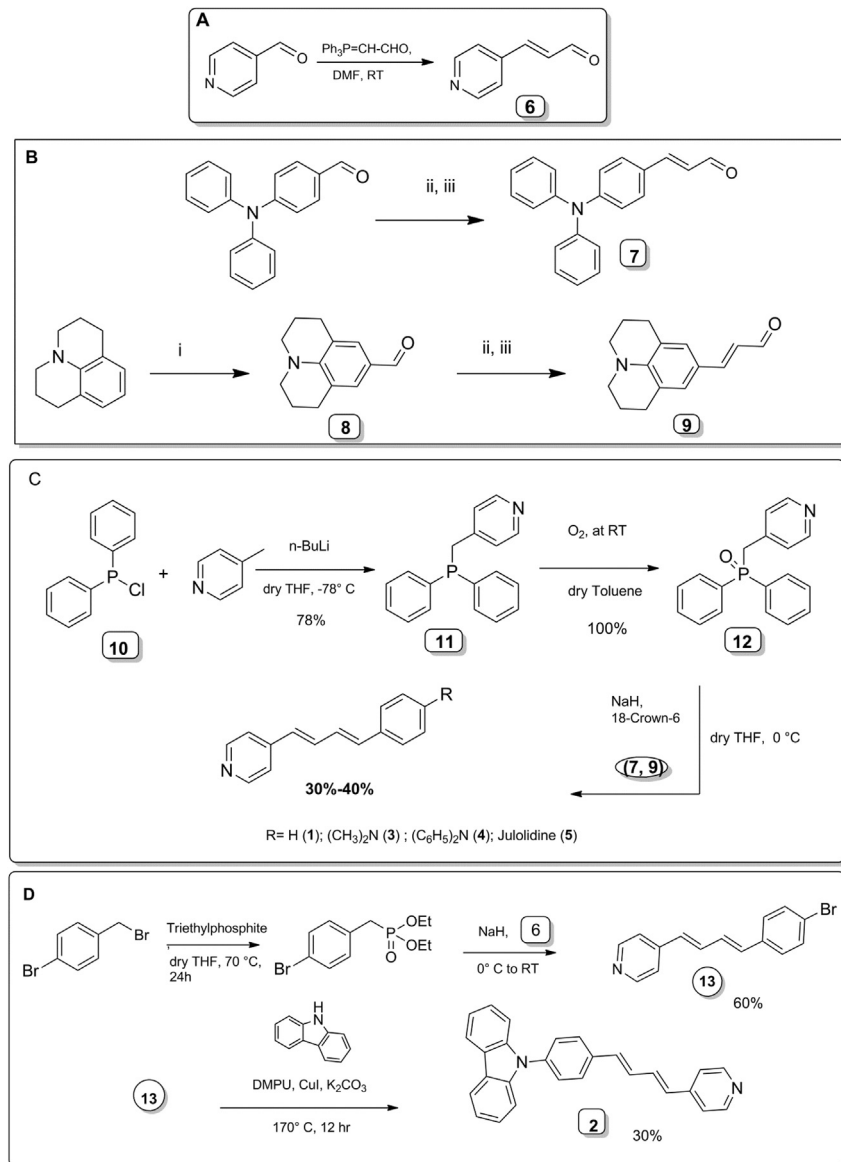
## 2.3. Synthesis of 9-((1E,3E)-4-(pyridin-4-yl)buta-1,3-dien-1-yl) phenyl-9H-carbazole (2)

Derivative (2) was synthesized by a method [35] showed in Scheme 1d. A mixture of carbazole (60 mg, 0.350 mmol), 4-((1E,3E)-4-(4-bromophenyl)buta-1,3-dienyl) pyridine diene (13) (100 mg, 0.350 mmol), CuI (0.0350 mmol), 18-Crown-6 (0.012 mmol),  $\text{K}_2\text{CO}_3$  (100 mg, 0.7 mmol) and 1 ml of 1,3-Dimethyl-3,4,5,6-tetrahydro-2(1H)-pyrimidinone (DMPU) was put into a round bottom flask, and then heated at 170 °C for 13 h under nitrogen atmosphere. After cooling to room temperature, the mixture was quenched with 1 N HCl, and the precipitate was washed with  $\text{NH}_3\text{--H}_2\text{O}$  and water. The residue was extracted with ethyl acetate, dried over  $\text{Na}_2\text{SO}_4$  and then concentrated under vacuum. The reaction mixture was purified on silica-gel column chromatography using 35% ethylacetate/hexane as eluent.

Characterization data: Orange solid  $^1\text{H}$  NMR ( $\text{CDCl}_3$ , 500 MHz, ppm)  $\delta$  8.57 (m, 2H),  $\delta$  8.15–8.14 (d, 2H),  $\delta$  7.69–7.67 (d, 2H),  $\delta$  7.57–7.56 (d, 2H), 7.46–7.40 (m, 4H), 7.31–7.29 (m, 4H), 7.21–7.16 (m, 1H,  $J = 15.5$  Hz), 7.07–7.02 (m, 1H,  $J = 15.5$  Hz), 6.89–6.85 (d, 1H,  $J = 15.5$  Hz), 6.66–6.62 (d, 1H,  $J = 15.5$  Hz);  $^{13}\text{C}$  NMR ( $\text{CDCl}_3$ , 125 MHz, ppm)  $\delta$  151.73, 150.21, 144.48, 140.69, 137.49, 135.83, 134.63, 133.34, 130.37, 128.93, 128.03, 127.21, 126.00, 123.51, 120.70, 120.36, 120.11, 109.79. HRMS [M+1]<sup>+</sup> 373.1699.

## 2.4. Computational details

Density functional theory (DFT) calculations have been performed using Gaussian 09 *ab initio* quantum chemical software package. DFT has been used for the ground-state properties and time-dependent DFT (TDDFT) for the estimation of ground to excited-state transitions. The geometry optimization of the molecules obtained using non-local functional B3LYP with 6-31G (d, p) basis set without any symmetry constraints. The minimized geometry was further confirmed by vibrational analysis, resulting in no imaginary frequencies and used as the input for further calculations to obtain the frontier molecular orbitals (FMOs) and single-point TDDFT studies (first 15 vertical singlet–singlet transitions) to obtain the UV–Vis spectra. The integral equation formalism polarizable continuum model (PCM) within the self-consistent reaction field (SCRF) theory, has been used for TDDFT calculations to describe the solvation of the dye in acetonitrile solvent. The



**Scheme 1.** Synthetic steps for preparation of dienes (1)–(5). Reagents and conditions: (i) (a) dry DMF, addition of POCl<sub>3</sub> at 0 °C. (b) after 30 min at 90 °C for 3 h (ii) 1,3-dioxan-2-yltributylphosphonium bromide, NaH, 18-crown-6, dry THF, RT, 24 h. (iii) 10% HCl, THF at RT, 1 h.

software GaussSum 2.2.5 was employed to simulate the major portion of the absorption spectrum and to interpret the nature of transitions.

### 3. Results and discussion

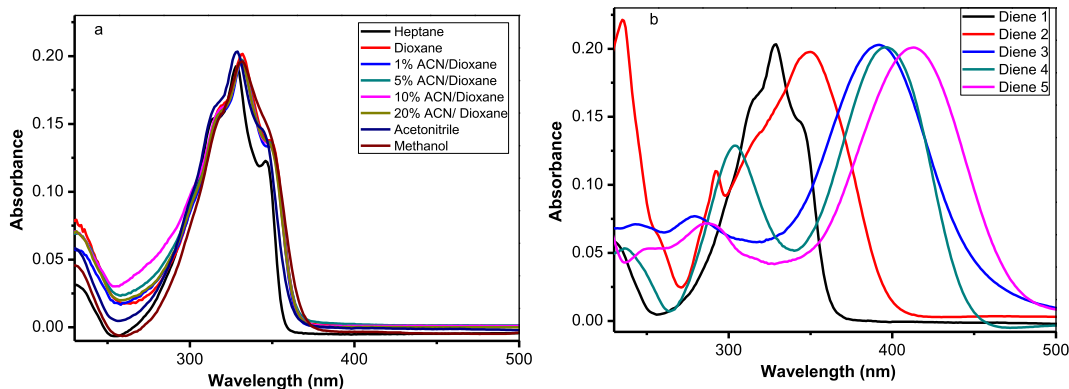
#### 3.1. Absorption and fluorescence properties

**Fig. 1** gives structural details of the dienes investigated. Diene (1) is a simple un-substituted 4-pyridyl-4-phenylbutadiene derivative. Diene (2) is substituted with carbazole while dienes (3), (4) and (5) have dimethylamine, diphenylamine and julolidine substituents respectively. These amino derivatives function as electron donors while the heterocyclic pyridine ring behaves as the electron acceptor. **Table 1** summarizes the absorption and fluorescence data of dienes (1–5) in different solvents. The absorption spectrum of diene (1) in different solvents is shown in **Fig. 2a**. This unsubstituted diene absorbs ( $\lambda_a$ ) at ~332 nm in acetonitrile. Upon introduction of electron donating moieties, significant absorption

changes are observed. The lowest shift (+18 nm) is obtained for diene (2) containing a carbazole group and a maximum shift (+81 nm) was observed for diene (5) containing julolidine [Fig. 2b]. Despite increase in the electron donating strength, only a small (+4 nm) wavelength shift was observed for diene (4) as compared to diene (3). This small increase is due to sharing of the lone pair of electrons on nitrogen between the adjacent phenyl rings and rest of the molecule. In case of diene (2), the carbazole ring system twists out of the plane with respect to the aryl group resulting in decreased electron donating strength. The absorption at ~300 nm in dienes (2) and (4) is attributed to the  $\pi-\pi^*$  transition of the triphenylamine or carbazole moiety. The other band located at about 360–390 nm with stronger intensity is due to the intramolecular charge transfer (ICT) absorption band [Fig. 2b and Fig. S2]. The alkyl substitution on nitrogen (5) increases the donating capacity through positive inductive effect (+I) effect resulting in larger absorption shifts. The possibility of planarization in the system is also another contributing factor [36]. Based on the observed absorbance data, the strength of electron donors can be

**Table 1**Absorption and emission data of diene (**1–5**) in various nonpolar to polar solvents.

Solvent	$\lambda_a$ (nm)	$\lambda_f$ (nm)	Stokes shift (cm <sup>-1</sup> )	$\Phi_f$	$\lambda_a$ (nm)	$\lambda_f$ (nm)	Stokes shift (cm <sup>-1</sup> )	$\Phi_f$
(2)								
Heptane	360	392	2267	0.78	383	446	3678	0.023
Dioxane (D)	356	436	5154	0.55	392	488	4019	0.021
1% AcN/D	356	439	5310	0.47	393	495	5243	0.017
5% AcN/D	356	445	5618	0.50	393	504	5604	0.019
10% AcN/D	355	454	6063	0.50	392	508	5825	0.019
20% AcN/D	354	460	6409	0.45	394	522	6223	0.019
AcN	350	492	8246	0.32	392	540	6992	0.018
Methanol	353	496	8167	0.02	394	551	7232	0.016
(3)								
Heptane	393	472	4259	0.40	403	442	2189	0.033
Dioxane (D)	395	481	4526	0.30	413	518	4998	0.031
1% AcN/D <sup>a</sup>	397	491	4822	0.16	—	—	—	0.031
5% AcN/D	397	498	5108	0.17	414	520	4924	0.032
10% AcN/D	396	504	5411	0.17	414	530	5387	0.033
20% AcN/D	397	513	5695	0.15	416	547	5757	0.035
AcN	396	534	6526	0.16	413	569	6639	0.034
Methanol	399	540	6544	0.02	419	583	6714	0.016
(4)								
Heptane	393	472	4259	0.40	403	442	2189	0.033
Dioxane (D)	395	481	4526	0.30	413	518	4998	0.031
1% AcN/D <sup>a</sup>	397	491	4822	0.16	—	—	—	0.031
5% AcN/D	397	498	5108	0.17	414	520	4924	0.032
10% AcN/D	396	504	5411	0.17	414	530	5387	0.033
20% AcN/D	397	513	5695	0.15	416	547	5757	0.035
AcN	396	534	6526	0.16	413	569	6639	0.034
Methanol	399	540	6544	0.02	419	583	6714	0.016
(5)								
Heptane	393	472	4259	0.40	403	442	2189	0.033
Dioxane (D)	395	481	4526	0.30	413	518	4998	0.031
1% AcN/D <sup>a</sup>	397	491	4822	0.16	—	—	—	0.031
5% AcN/D	397	498	5108	0.17	414	520	4924	0.032
10% AcN/D	396	504	5411	0.17	414	530	5387	0.033
20% AcN/D	397	513	5695	0.15	416	547	5757	0.035
AcN	396	534	6526	0.16	413	569	6639	0.034
Methanol	399	540	6544	0.02	419	583	6714	0.016

<sup>a</sup> AcN is acetonitrile. Quinine sulfate (0.545 in 0.5 N H<sub>2</sub>SO<sub>4</sub> is used as standard).**Fig. 2.** Normalized UV spectra of (a): (**1**) in varying solvent polarity; (b): (**1–5**) in acetonitrile (ACN is acetonitrile).

given as H < Carbazole < N, N-dimethyl ≤ N, N-diphenyl < Julolidine.

The dienes show vibrational structure in non-polar heptane and a smooth structure less absorption spectrum in solvents of higher polarity. This is attributed to involvement of charge transfer and strong solute–solvent interactions. Solvent polarity variations lead to small absorption wavelength shifts (~4–16 nm) [Fig. 2b and Fig. S1 & S2]. Among the dienes, (**5**) shows a maximum shift of 16 nm from non-polar heptane to acetonitrile, and carbazole containing (**2**) shows an absorption shift of about 7 nm.

To understand the effect of the amino donating groups on electronic, optical and geometrical properties of the dienes (**1–5**), density functional theory (DFT) calculations were performed using Gaussian 09 *ab initio* quantum chemical software package. The optimized geometry with dihedral angles, molecular orbital amplitude plot of the highest occupied molecular orbitals (HOMOs) and lowest unoccupied molecular orbitals (LUMOs) of the dienes (**1–5**) are shown in Fig. 3. The optimized geometries obtained from B3LYP/6-31g (d, p) level of theory shows that all the dienes except (**2 & 4**) are almost planar in nature. In diene (**2**), carbazole is twisted out of the plane of the diene system with the dihedral angle of 54.1°. Similarly in diene (**4**), a large torsion angle of ~47° observed between the phenyl rings present in the starburst triphenylamine (TPA) segment. The steric repulsion induced by the diphenylamine unit in TPA derivative twisted out the plane of the diene system to the dihedral angle of 37.1°. This out of plane twisting results in

lowered absorption maxima, contrary to expected absorption maxima based solely on electron donating strength. This is substantiated from TDDFT simulation studies. In all the molecules, the HOMOs are completely delocalized over the entire molecule, whereas the LUMOs are mainly populated over the unsaturated chain and the pyridine unit. This charge separation observed from the distribution of HOMO and LUMO indicates that the HOMO→LUMO transition bears a considerable intramolecular charge-transfer (ICT) character.

TDDFT calculations were used to examine the vertical excitation energy of the dienes using B3LYP functional. The absorption spectra show a small underestimation in gas phase (not shown) and used the same functional further in the framework of polarizable continuum model (PCM) with acetonitrile as solvent. The trend in these computed values is in reasonable agreement with the experimentally observed wavelength maximum. The plot of TDDFT simulated spectra of the dienes (**1–5**) is depicted in Fig. 4. The comparison of computed HOMO-LUMO energy difference, lowest excitation energies along with their oscillator strength, nature of transitions and the ground state dipole moment of all the dienes using the B3LYP level of theory with experimental observations were summarized in Table S1. The relative tendency in the absorption wavelength is interpreted by means of molecular orbitals composition which is essential to determine the extent of charge-separation. The HOMO to LUMO transition for all the dienes (**1–5**) are calculated to be 97%, 79%, 93%, 86% and 92% respectively.

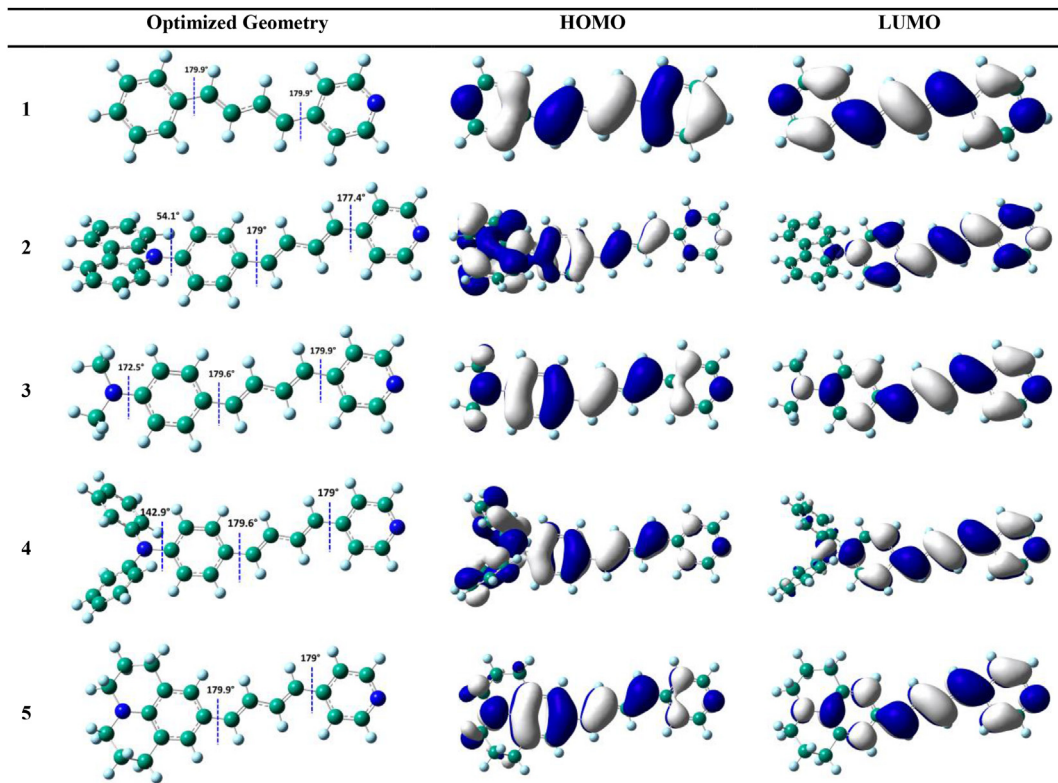


Fig. 3. Optimized geometries and their computed isodensity (0.02) surfaces of HOMO and LUMO of the dienes (1)–(5).

Dienes (**2**–**5**) show considerable ICT nature besides  $\pi$ - $\pi^*$  transition, whereas in diene (**1**),  $\pi$ - $\pi^*$  transition is more predominant [37,38]. It is worth noting that the HOMO to LUMO transition of dienes (**2**) and (**4**) containing carbazole and triphenylamine as electron donors are comparatively lower (Table S1). This may be attributed to the non-planar donor-acceptor interaction which leads to poor overlap of orbital interactions over the system.

### 3.2. Fluorescence properties in solution

Table 1 detail the absorption and fluorescence data of the investigated dienes. Diene (**1**) has very weak fluorescence and the spectrum is highly noisy (Fig. S3). The weak emission is due to fast deactivation of the molecules in the excited state through free rotation of the molecules as the excited state has less double bond

character compared to the ground state processes and also due to strong non-radiative losses through processes such as internal conversion [39,40]. In comparison, the amino derivatives (**2**–**5**) generally result in broad, structure-less emission band with strong solvatochromic emission shifts ( $\lambda_f$ ) with the increase in solvent polarity. Among the dienes investigated, diene (**5**) containing the julolidine group has a maximum bathochromic shift (+141 nm) from heptane to acetonitrile while diene (**4**) bearing a diphenylamino group leads to a minimum (+68 nm) shift [Fig. 5]. The enhanced strength of electron donating group due to the presence of alkyl groups in julolidine result in huge solvatochromic emission shifts. Such a large solvatochromic shifts observed can be attributed to twisted intramolecular charge transfer (TICT) and this attribute was utilized as viscosity or polarity dependent fluorescence probes [41,42]. Diene (**3**), with dimethylamino groups also exhibit large solvent polarity dependent emission shifts. In comparison, a related derivative of (**3**) containing a phenyl ring in place of a pyridine ring shows an emission shift of 56 nm [43]. Despite twisting out of plane, carbazole containing diene (**2**) shows a bathochromic shift of ~100 nm. This strong bathochromic shift in dienes clearly shows that fluorescence originates as a consequence of pronounced increase in charge separation due to intramolecular charge transfer (ICT). This ICT state was also reflected through observance of large a Stokes shift for these dienes in polar solvents. Large Stokes shift indicates least overlap of absorption and emission and this characteristic enables their use as biological labels [44]. Among the dienes, (**2**) containing carbazole exhibits larger Stokes shift as compared to other dienes. Although more twisting was expected in carbazole substituted compound, it can experience large electron delocalization resulting in a greater ICT character [45]. The calculated quantum yields are also higher for carbazole containing (**2**) than other dienes. The quantum yields for diphenylamine containing (**4**) are also higher indicating the potential utility of these

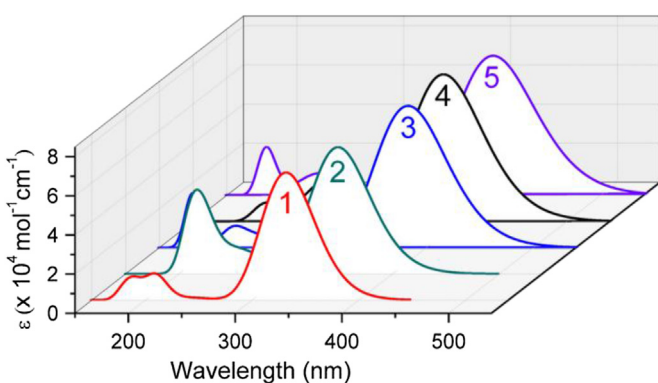
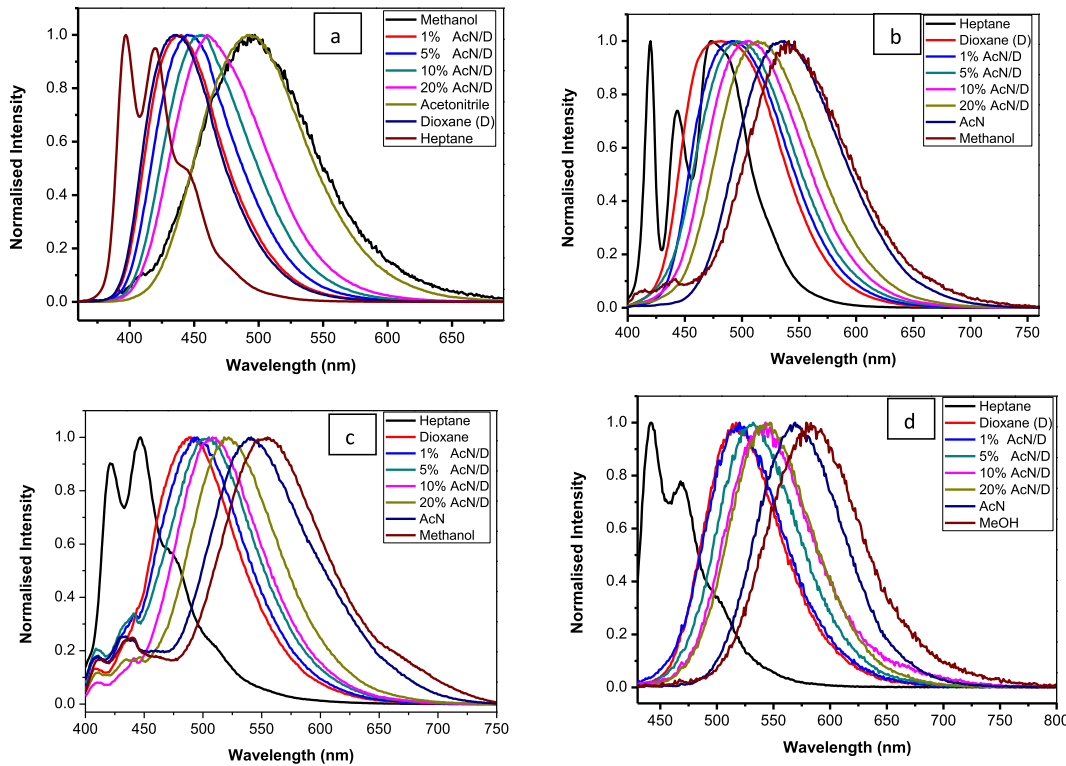


Fig. 4. Simulated absorption spectra obtained with TD-DFT/B3LYP/6-31G (d, p) level of theory.



**Fig. 5.** Emission spectra of (a) **2**, (b) **4**, (c) **3** and (d) **5**.

chromophores for biological or optical applications. The dienes containing aliphatic amino substitutions (**3** and **5**) both show lower quantum yield of fluorescence. Despite the restriction caused by the aliphatic ring, diene (**5**) shows comparable quantum yields with diene (**3**). To further examine the solvatochromic shift, the excited state dipole moment ( $\mu_e$ ) of dienes (**2–5**) was calculated using Lippert–Mataga equation [46]. The dipole moment ( $\mu_e$ ) of the ICT excited states can be calculated from the slope ( $m_f$ ) of the plot of the Stokes shift with  $\Delta f$  according to eq

$$\nu_{ss} = \left[ 2(\mu_e - \mu_g)^2 / hca^3 \right] \Delta f + \nu_{ss0}$$

where,  $\nu_{ss}$  is the Stokes shift,  $\mu_g$  is the ground state dipole moment and were obtained using DFT calculations utilizing Gaussian Software,  $a$  is the solvent cavity (Onsager) radius. The solvent parameter  $\Delta f$  represents solvent polarity and polarizability and defined as

$$\Delta f = [(\epsilon - 1)] / (2\epsilon + 1) - \left[ (n^2 - 1) / (2n^2 + 1) \right]$$

where  $\epsilon$  and  $n$  are solvent dielectric constant and refractive index respectively. The Onsager radius ( $a$ ) calculated by the formula

$$a = (3M/4N\pi d)^{1/3}$$

**Table 2**

Calculated Onsager radius, slope of the curve, ground and excited state dipole moments of dienes investigated.

Compound	$a(\text{\AA})$	$m_f$	$\mu_g(\text{D})$	$\mu_e(\text{D})$
<b>2</b>	5.28	10,924	1.8522	$14.47 \pm 0.014$
<b>3</b>	4.63	7982	7.6166	$16.47 \pm 0.022$
<b>4</b>	5.28	7346	5.0880	$15.45 \pm 0.005$
<b>5</b>	4.93	6569	8.3659	$17.18 \pm 0.022$

In this, (N) is Avogadro number, (M) is the molecular weight, and (d) is the density and taken as 1 g/cm<sup>3</sup> [47]. The estimated dipole moments ( $\mu_e$ ) are listed in Table 2 along with calculated values of  $a$ ,  $m_f$ ,  $\mu_g$ , for dienes (**2–5**). The plots of  $\Delta\nu(v_A - v_F)$  vs  $\Delta f$  are shown in Fig. S4. In all the cases, a linear correlation with a positive solvatochromism was observed indicating their solvent sensitive behavior due to presence of intramolecular charge transfer (ICT) emissive states.

The ICT state is also reflected by large change in excited state dipole moment. The ICT states of diene (**2–5**) have larger dipole moments in the excited state than in the ground state as a result of the charge separation between the donor and acceptors. The order of  $\mu_e$  is (**5**) > (**3**) > (**4**) > (**2**). The observed excited state dipole moments confirm the earlier observations of greater charge transfer character for julolidine substituted diene (**5**). The competing processes of sharing of lone pair of electrons in (**2**) and (**4**) and the bulkier donating groups in the form of triphenylamine

**Table 3**

Fluorescence lifetime data in homogeneous solvents. Diene (**2**) was excited at 360 nm. Diene (**3**), (**4**) and (**5**) were excited at 405 nm (error percentage-0.1–0.3%).

Diene	Solvent	$\tau_1$	$\tau_2$	$\chi^2$
<b>(2)</b>	Dioxane	1.32	—	1.03
	20% ACN/Dioxane	1.87	—	1.08
	Acetonitrile	2.52	—	1.04
<b>(3)</b>	Dioxane	0.11 (98.49%)	1.13 (1.51%)	0.86
	20% ACN/Dioxane	0.16 (90.89%)	0.54 (8.70%)	0.88
	Acetonitrile	0.18 (91.75%)	0.50 (7.87%)	0.88
<b>(4)</b>	Dioxane	1.24	—	0.92
	20% ACN/Dioxane	1.53	—	1.04
	Acetonitrile	1.82	—	0.90
<b>(5)</b>	Dioxane	0.25 (91.14%)	2.50 (8.86%)	0.97
	20% ACN/Dioxane	0.47 (97.03%)	2.53 (2.96%)	1.02
	Acetonitrile	0.57 (99.80%)	2.77 (0.20%)	0.90

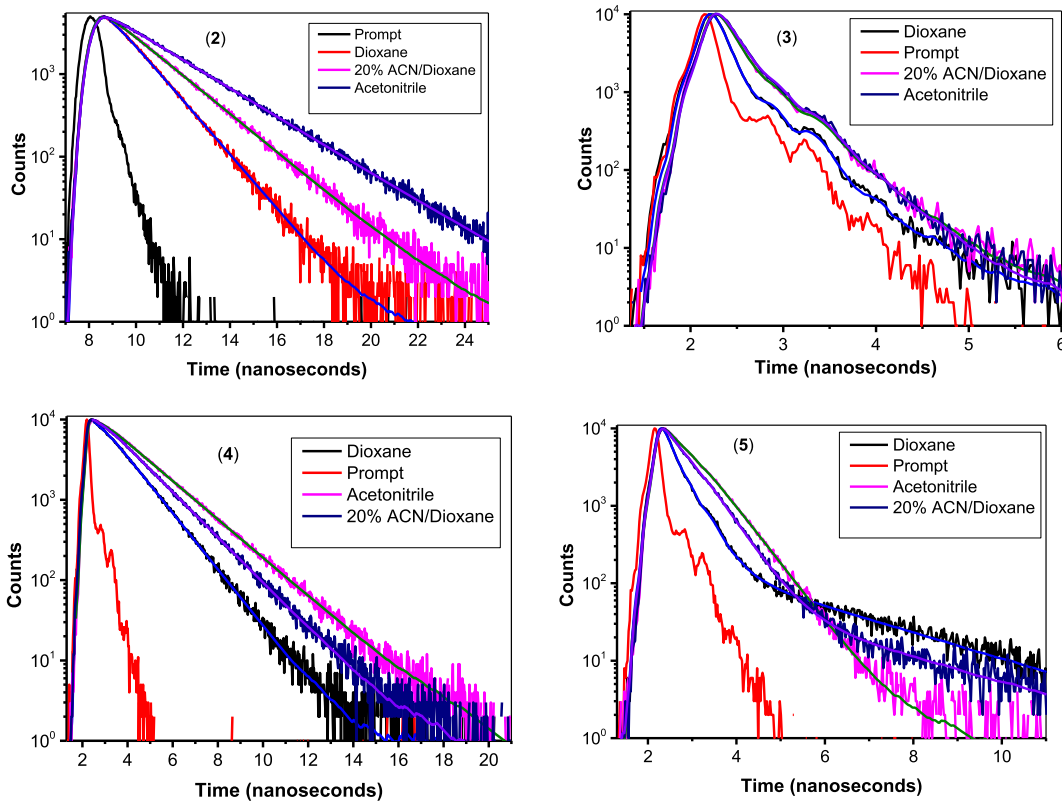


**Fig. 6.** Excited state decay profile of dienes (2–5) in different solvents. Excitation of 360 nm for (2) and (b) 405 nm for (3–5).

and carbazole lead to reduction in electron delocalization in excited state and therefore result in decreased  $\mu_e$  values in comparison to (3) and (5). The presence of alkyl (methyl) groups on nitrogen facilitates the availability of electrons for electron charge transfer during the excited state resulting in increase in  $\mu_e$  for diene (3) and (5).

Room temperature lifetimes of dienes in different solvents are shown in Table 3. Dienes (2) and (4) bearing carbazole and triphenylamine moieties show single exponential decay while dienes (3) and (5) show bi-exponential decay with major component having population greater than 90% with lifetime in the range of 0.11 ns–0.57 ns. The minor component (with a population less than 10%) has a lifetime in the range of 0.50 ns–2.77 ns. It is possible that both the dienes containing dimethylamino and julolidine have excited states that contribute to conformational changes due to their significant intramolecular charge transfer nature [Fig. 6]. Thus it can be said that the fluorescence majorly originates from a single excited state species in the case of (2) and (4) but originates from two excited states in the case of (3) and (5) due to conformational changes. Such biexponential decay is also reported in similarly substituted stilbene derivative [48].

#### 4. Conclusions

In summary, we have designed and synthesized arylbutadienes containing different amino substituted derivatives as electron-donating groups and pyridine as an electron-accepting group. Their excited state properties are strongly solvent-dependent, while their absorption spectra show moderate changes in various solvents. The nature of electron donating group markedly influences the emission shifts with julolidine electron-donating substituent causing greater red-shift of the fluorescence

maximum, indicating efficient intramolecular charge transfer behavior. It can further be proposed from these studies that such strongly solvatochromic probes can be useful materials for optical and biological applications.

#### Acknowledgements

Authors gratefully thank CSIR [Grant no: 01(2487)/11/EMR-II], Department of Science and Technology and IIT Gandhinagar for research support.

#### Appendix A. Supplementary data

Supplementary data related to this article can be found at <http://dx.doi.org/10.1016/j.dyepig.2015.08.018>.

#### References

- [1] Roncali J, Leriche P, Blanchard P. Molecular materials for organic photovoltaics: small is beautiful. *Adv Mater* 2014;26:3821–38.
- [2] Babu SS, Praveen VK, Ajayaghosh A. Functional  $\pi$ -gelators and their applications. *Chem Rev* 2014;114:1973–2129.
- [3] Beverina L, Pagani GA.  $\pi$ -conjugated zwitterions as paradigm of donor–acceptor building blocks in organic-based materials. *Acc Chem Res* 2013;47:319–29.
- [4] Li Y, Liu T, Liu H, Tian M-Z, Li Y. Self-assembly of intramolecular charge-transfer compounds into functional molecular systems. *Acc Chem Res* 2014;47:1186–98.
- [5] Xu J, Semin S, Rasing T, Rowan AE. Organized chromophoric assemblies for nonlinear optical materials: towards (Sub) wavelength scale architectures. *Small* 2015;11:1113–29.
- [6] Müller TJJ, Bunz UHF. Functional organic materials: syntheses, strategies and applications. John Wiley & Sons; 2007.
- [7] Mizukami W, Kurashige Y, Ehara M, Yanai T, Itoh T. Ab initio study of the excited singlet states of all-trans, $\omega$ -diphenylpolyenes with one to seven polyene double bonds: simulation of the spectral data within Franck–Condon approximation. *J Chem Phys* 2009;131:1734313.

- [8] Shin DM, Whitten DG. Solvatochromic behavior of intramolecular charge-transfer diphenylpolyenes in homogeneous solution and microheterogeneous media. *J Phys Chem* 1988;92:2945–56.
- [9] Baraldi I, Spalletti A, Vanossi D. Rotamerism and electronic spectra of azaderivatives of stilbene and diphenylbutadiene. A combined experimental and theoretical study. *Spectrochim Acta A* 2003;59A:75–86.
- [10] Eastman Jr LR, Zarnegar BM, Butler JM, Whitten DG. Unusual case of selectivity in a photochemical reaction. Photoisomerization of unsymmetrical 1,3-dienes. *J Am Chem Soc* 1974;96:2281–3.
- [11] Bartocci G, Galiazzo G, Latterini L, Marri E, Mazzucato U, Spalletti A. Photoisomerization mechanisms and photoselectivity of the stereoisomers of 1-(pyrid-n-yl)-4-phenylbuta-1,3-diene. *Phys Chem Chem Phys* 2002;4:2911–6.
- [12] Redwood CE, Kanval S, Samudrala R, Saltiel J. Bicycle pedal photoisomerization of 1-phenyl-4-(4-pyridyl)-1,3-butadienes in glassy isopentane at 77. *Photochem Photobiol Sci* 2013;12:1754–60.
- [13] Bartocci G, Galiazzo G, Gennari G, Marri E, Mazzucato U, Spalletti A. Effect of the nature of aryl and heteroaryl groups on the excited state properties of asymmetric 1,4-diarylbisubdienes. *Chem Phys* 2001;272:213–25.
- [14] Bartocci G, Galiazzo G, Mazzucato U, Spalletti A. Photophysics and photochemistry of the EE and ZE isomers of 1-(n-pyridyl)-4-phenyl-1,3-butadiene ( $n = 2, 3$  and 4). *Phys Chem Chem Phys* 2001;3:379–86.
- [15] Kumar NSS, Varghese S, Rath NP, Das S. Solid state optical properties of 4-alkoxy-pyridine butadiene derivatives: reversible thermal switching of luminescence. *J Phys Chem C* 2008;112:8429–37.
- [16] Yamada S, Azuma Y, Aya K. [2+2] photodimerization of 1-aryl-4-pyridylbutadienes through cation–π interactions. *Tet Lett* 2014;55:2801–4.
- [17] Nakamura A, Irie H, Hara S, Sugawara M, Yamada S. Regiospecific [2 + 2] photocyclodimerization of trans-4-styrylpyridines templated by cucurbit[8]uril. *Photochem Photobiol Sci* 2011;10:1496–500.
- [18] Gao X, Friscic T, MacGillivray LR. Supramolecular construction of molecular ladders in the solid state. *Angew Chem Int Ed* 2003;43:232–6.
- [19] Ooyama Y, Inoue S, Nagano T, Kushimoto K, Ohshita J, Imae I, et al. Dye-sensitized solar cells based on donor–acceptor π-conjugated fluorescent dyes with a pyridine ring as an electron-withdrawing anchoring group. *Angew Chem Int Ed* 2011;50:7429–33.
- [20] Ooyama Y, Nagano T, Inoue S, Imae I, Komaguchi K, Ohshita J, et al. Dye-Sensitized solar cells based on donor–π-acceptor fluorescent dyes with a pyridine ring as an electron-withdrawing anchoring group. *Chem Eur J* 2011;17:14837–43.
- [21] Cui J, Lu J, Xu X, Cao K, Wang Z, Alemu G, et al. Organic sensitizers with pyridine ring anchoring group for p-type dye-sensitized solar cells. *J Phys Chem C* 2014;118:16433–40.
- [22] Tessore F, Cariati E, Cariati F, Roberto D, Ugo R, Mussini P, et al. The role of ion pairs in the second-order NLO response of 4-X-1-methylpyridinium salts. *Chem Phys Chem* 2010;11:495–507.
- [23] Brown AS, Bernal L-M, Micotto TL, Smith EL, Wilson JN. Fluorescent neuroactive probes based on stilbazolium dyes. *Org Biomol Chem* 2011;9:2142–8.
- [24] Wilson JN, Brown AS, Babinchak WM, Ridge CD, Walls JD. Fluorescent stilbazolium dyes as probes of the norepinephrine transporter: structural insights into substrate binding. *Org Biomol Chem* 2012;10:8710–9.
- [25] Amaral E, Guatimosim S, Guatimosim C. Using the fluorescent styryl dye FM1-43 to visualize synaptic vesicles exocytosis and endocytosis in motor nerve terminals. In: Chiarini-Garcia H, Melo RCN, editors. Light microscopy. Humana Press; 2011. p. 137–48.
- [26] Mazzoli A, Carlotti B, Consiglio G, Fortuna CG, Miolo G, Spalletti A. Photo-behaviour of methyl-pyridinium and quinolinium iodide derivatives, free and complexed with DNA. A case of bisintercalation. *Photochem Photobiol Sci* 2014;13:939–50.
- [27] Mazzoli A, Carlotti B, Bonaccorso C, Fortuna CG, Mazzucato U, Miolo G, et al. Photochemistry and DNA-affinity of some pyrimidine-substituted styryl-azinium iodides. *Photochem Photobiol Sci* 2011;10:1830–6.
- [28] Krieg R, Eitner A, Guenther W, Schuerer C, Lindenau J, Halbhuber KJ. N,N-dialkylaminostyryl dyes: specific and highly fluorescent substrates of peroxidase and their application in histochemistry. *J Mol Histol* 2008;39:169–91.
- [29] Coe BJ, Harris JA, Asselberghs I, Wostyn K, Clays K, Persoons A, et al. Quadratic optical nonlinearities of N-methyl and N-aryl pyridinium salts. *Adv Funct Mater* 2003;13:347–57.
- [30] Kuzyl MG. Using fundamental principles to understand and optimize nonlinear-optical materials. *J Mater Chem* 2009;19:7444–65.
- [31] Russo SF. Two fluorescence experiments. *J Chem Educ* 1969;46:374.
- [32] Palatinus L, Chapuis G. SUPERFLIP—a computer program for the solution of crystal structures by charge flipping in arbitrary dimensions. *J Appl Crystallogr* 2007;40(4):786–90.
- [33] Hubschle CB, Sheldrick GM, Dittrich B. ShelXle: a Qt graphical user interface for SHELXL. *J Appl Crystallogr* 2011;44:1281–4.
- [34] Hung-Low F, Klausmeyer KK, Gary JB. Effect of anion and ligand ratio in self-assembled silver(I) complexes of 4-(diphenylphosphinomethyl)pyridine and their derivatives with bipyridine ligands. *Inorg Chim Acta* 2009;362:426–36.
- [35] Xu Q-L, Li H-Y, Wang C-C, Zhang S, Li T-Y, Jing Y-M, et al. Synthesis, structure, photophysical and electrochemical properties of series of new fac-tricyclometallated iridium complexes with carbazole or oxadiazole moieties. *Inorg Chim Acta* 2012;391:50–7.
- [36] Letard JF, Lapouyade R, Rettig W. Structure–photophysics correlations in a series of 4-(dialkylamino) stilbenes: intramolecular charge transfer in the excited state as related to the twist around the single bonds. *J Am Chem Soc* 1993;115:2441–7.
- [37] Vivas MG, Silva DL, Malinge J, Boujtita M, Zalešny R, Bartkowiak W, et al. Molecular structure – optical property relationships for a series of non-centrosymmetric two-photon absorbing push-pull triarylamine molecules. *Sci Rep* 2014;4:1–11.
- [38] Huang T-H, Hou J-Q, Kang Z-H, Wang Y-H, Lu R, Zhou H-P, et al. Investigation on the linear and nonlinear optical properties of fluorenone-based linear conjugated oligomers: the influence of π-spacer. *J Photochem Photobiol A Chem* 2013;261:41–5.
- [39] Marconi G, Bartocci G, Mazzucato U, Spalletti A, Abbate F, Angeloni L, et al. Role of internal conversion on the excited state properties of trans-styrylpuridines. *Chem Phys* 1995;196:383–93.
- [40] Spalletti A, Bartocci G, Elisei F, Masetti F, Mazzucato U. Effect of pyridyl and thiényl groups on the excited state properties of stilbene-like molecules. *Proc Ind Acad Sci* 1998;110:297–310.
- [41] Goh WL, Lee MY, Joseph TL, Quah ST, Brown CJ, Verma C, et al. Molecular rotors as conditionally fluorescent labels for rapid detection of biomolecular interactions. *J Am Chem Soc* 2014;136:6159–62.
- [42] Martini G, Martinelli E, Ruggeri G, Galli G, Pucci A. Julolidine fluorescent molecular rotors as vapour sensing probes in polystyrene films. *Dyes Pigm* 2015;113:47–54.
- [43] Singh AK, Darshi M. Fluorescence probe properties of intramolecular charge transfer diphenylbutadienes in micelles and vesicles. *Biochim Biophys Acta* 2002;1563:35–44.
- [44] Xue L, Liu C, Jiang H. A ratiometric fluorescent sensor with a large stokes shift for imaging zinc ions in living cells. *Chem Commun* 2009;1061–3.
- [45] H-p Shi, Xu L, Cheng Y, He J-y, Dai J-x, Xing L-w, et al. Experimental and theoretical study of three new benzothiazole-fused carbazole derivatives. *Spectrochim Acta Part A* 2011;81:730–8.
- [46] Lakowicz JR. Principles of fluorescence spectroscopy. Springer Science & Business Media; 2007.
- [47] Yang J-S, Lin C-K, Lahoti AM, Tseng C-K, Liu Y-H, Lee G-H, et al. Effect of ground-state twisting on the trans → cis photoisomerization and TICT state formation of aminostilbenes. *J Phys Chem A* 2009;113:4868–77.
- [48] Sowmiya M, Tiwari AK, Sonu, Saha SK. Study on intramolecular charge transfer fluorescence properties of trans-4-[4'-(N,N'-dimethylamino)styryl] pyridine: effect of solvent and pH. *J Photochem Photobiol A Chem* 2011;218:76–86.